atmosphere

MDPI

Article

Re-Engineering Dew-Harvesting Cactus Macrostructures to Enhance Water Collection as an Adaptive Climate Change Strategy: An Experimental Comparison

Tegwen Malik [1,2,*], David Gethin [3], Frederic Boy [1,4], Gareth Davies [1] and Andrew Parker [5]

[1] i-Lab Research Centre, School of Management, Swansea University, Swansea SA1 8EN, UK; f.a.boy@swansea.ac.uk (F.B.)
[2] Climate Action Research Institute (CARI), Swansea University, Swansea SA1 8EN, UK
[3] College of Engineering, Swansea University, Swansea SA1 8EN, UK
[4] Zienkiewicz Institute for Modelling and AI, Faculty of Science and Engineering, Swansea University, Swansea SA1 8EN, UK
[5] Green Templeton College, Oxford University, 43 Woodstock Road, Oxford OX2 6HG, UK
* Correspondence: f.t.malik@swansea.ac.uk

Abstract: The spinal structures found on *Copiapoa cinerea* var. *haseltoniana*, an efficient dew-harvesting cactus, were fabricated and evaluated both in a climate chamber and outdoors in dewy conditions. A mix of aluminium and steel was used to fabricate these surfaces, with aluminium being used for everything but the replicated spine features, which were constructed from steel. Each surface was entirely coated with a highly emissive paint containing an alumina–silicate OPUR additive. Three replica versions (stem only, spine only, and stem & spine) were compared to a flat planar reference surface. Experimental results demonstrated that all three biomimetic macro-structured surfaces significantly enhanced dew harvesting compared to the reference surface. It was established that the stem & spine replica, spine replica, and stem replica all demonstrated significantly more dew harvesting, with mean efficiency ratios in respect of the reference surface of 1.08 ± 0.03, 1.08 ± 0.02, and 1.02 ± 0.01, respectively. Furthermore, the method of surface water collection was found to influence the water collection rate. The diagonal run-off flow across a flat planar surface was 34% more efficient than the parallel run-off flow on the same surface. These findings provide valuable insights for the construction and installation of biomimetic-inspired dew-harvesting devices, particularly in regions that are most challenged by decreasing dew yields as a result of climate change.

Keywords: biomimetics; surface structures; cacti; water harvesting; climate change; dew; bio-inspiration

Citation: Malik, T.; Gethin, D.; Boy, F.; Davies, G.; Parker, A. Re-Engineering Dew-Harvesting Cactus Macrostructures to Enhance Water Collection as an Adaptive Climate Change Strategy: An Experimental Comparison. *Atmosphere* **2023**, *14*, 1736. https://doi.org/10.3390/atmos14121736

Academic Editors: Marc Muselli and Daniel Beysens

Received: 9 October 2023
Revised: 20 November 2023
Accepted: 23 November 2023
Published: 25 November 2023

1. Introduction

In the year 2000, the World Health Organization (WHO) declared that access to a clean water supply and sanitation was a fundamental human right [1], and that a deficiency in these areas had a significant negative impact on the health of a population. Fifty litres of safe water per person per day has been deemed necessary, and 3 litres per day is the minimal requirement to replace lost fluid in average climatic conditions [2]. While approximately 70% of the Earth is covered by water, only 2.5% is not salty (with two-thirds of this fresh water being not directly usable, tied up in glaciers or buried deep underground [3]. Thus, it is a paradox that the continuous water supply that most people in the developed world take for granted is seen through very different eyes in other regions, where climate and demographics apply an ever-increasing pressure on resources.

This growing water demand must be addressed sustainably to ensure water availability for essential purposes such as drinking, washing, cooking, cleaning, agriculture, livestock, and medicine. For these reasons, harvesting airborne moisture is deemed not only

a critical factor in addressing the growing demand for water but an exciting proposition, especially in arid regions. Potable water needs are essential all around the world, especially so in areas that are arid, such as the western United States, which has suffered from an unprecedented long-term drought [4]. Places such as California are trying to address this problem by looking at fog water using mesh–screed fog collectors [5]; this may not be the only solution, however, due to Californian fog being seasonal, and hence, the potential for harvesting dew is an important consideration. It has been predicted, however, that regions such as Northwestern Africa and the broader Mediterranean basin are projected to endure a significant decline in precipitation and dew yields as a result of climate change due to decreasing relative humidity [6,7]. It will thus become even more critical to enhance the performance of airborne moisture harvesters to adapt to the challenges faced due to climate change.

Dew harvesters or condensers have been optimized through "surface morphology" and optimizing wettability with higher dew droplet nucleation forming on hydrophilic surfaces rather than hydrophobic surfaces [8]. That said, nature's moisture harvesters have been shown to have, at times, a combination of hydrophilic and hydrophobic areas on their surfaces [9], with some in the field discussing the importance of hydrophobic substrates as also being important to consider when thinking about condensation [10]. The shape of condensers has also been deemed important, with studies improving the performance of condensers by making them funnel-shaped [11], as well as those with an origami-shaped surface along with an egg-box-shaped-surface condenser [12]. These studies found the funnel-shaped condenser (with a cone angle of approximately 60°) to be more efficient at harvesting dew than a planar condenser, and the origami to be the most efficient of all, with a strong correlation between how effectively a condenser cools and its subsequent dew yield. However, manufactured dew and fog harvesters have not been significantly influenced by nature, and the present research aims to bring such influences to bear on the subject where designs may be up-scaled through commercial fabrication routes.

It is only logical to conclude that plants and animals must have evolved to be able to gather the water necessary for survival in arid climates such as the Atacama and Namib Deserts. Highly regular macro-structures are commonly found in plants, forming patterns on their surfaces [13]. These regular plant structures are usually formed from leaves that grow from the stem of a plant; a phenomenon known in plant biology as phyllotaxis [14]. The leaves of cacti, however, are the spines, and it is these spines that are known to harvest airborne moisture [15–17]. Previous work in this area found the dew-harvesting efficiency of an Atacama Desert-dwelling cactus, *Copiapoa cinerea*, to be efficient, and that the presence of cacti spines increased the dew-harvesting efficiency of this particular species of cactus [18], with the spines of *C cinerea* directing dew droplets from their tips to their bases [19]. This species of cacti can be found growing on the coastal regions of the Atacama Desert (from sea level up to a height of 1300 m) between Tocopilla city and the slopes of the Choapa Valley [20]. The aims of the present research study, which forms part of a more comprehensive research project [21], was the first to replicate and fabricate the stem and spine geometry of *C. cinerea*, and secondly to assess whether geometrically replicated structures also increase dew-harvesting efficiency. It is hoped that this will feed into wider adaptive strategies enabling humans to access water under challenging climatic conditions.

2. Methods

Before examining the dew-harvesting efficiency on fabricated surfaces inspired by the macro-structures of the cactus *C. cinerea*, surface measurements were obtained from this species to establish a comprehensive understanding of its surface. Following these measurements, three surfaces were fabricated, incorporating stem structures, spine structures, and a combination of both. These surfaces were coated with a hydrophilic, highly emissive (in the infrared spectrum) paint known to enhance radiative cooling. The coating consisted of a mix of 15% OPUR (International Organization for Dew Utilization) alumina–silicate additive stirred into the topcoat paint. This additive, utilized in previous dew-harvesting

studies [22], ensures that the surface coating is hydrophilic and highly emissive. Other studies have achieved a coated surface of high IR emissivity while ensuring the wetting properties of the dew-harvesting surface are hydrophilic using OPUR foil [23,24], which was not practical in this particular study due to the complexity of the surface structures under investigation.

The OPUR paint mix coating also had the benefit of ensuring that all surfaces had the same surface chemistry/properties. The fabrication method was designed so that all the surfaces were made using the same materials to ensure consistency before carrying out indoor and outdoor measurements on them to assess their dew-harvesting efficiency. A flat reference surface was also made using the same materials and coating.

2.1. Macro Measurements of C. cinerea

The plant being replicated in this study was the same as that used by Malik et al. [18] and is shown in Figure 1. Average macro-measurements of this plant, *C. cinerea*, were taken, namely the spine length (8.6 mm $\pm$ 2.7 mm), spine base width (434 µm $\pm$ 77 µm), tip-to-tip spine spacing (8.4 mm $\pm$ 0.6 mm), and areole spacing on the plant stem, to be used when fabricating the surface. Typically, an areole is the peak of the bumps and ridges found on the cacti stems and are the part of the surface of the plants from which spines emanate. The angle measured showing the areole-to-areole arrangement of *C. cinerea*, along with the number of areoles in the 360° range around each areole, was typically found to be $\approx$60° $\pm$ 23°, with the average number of surrounding areoles therefore being six, and the distance between each areole was 8.7 mm $\pm$ 0.44 mm.

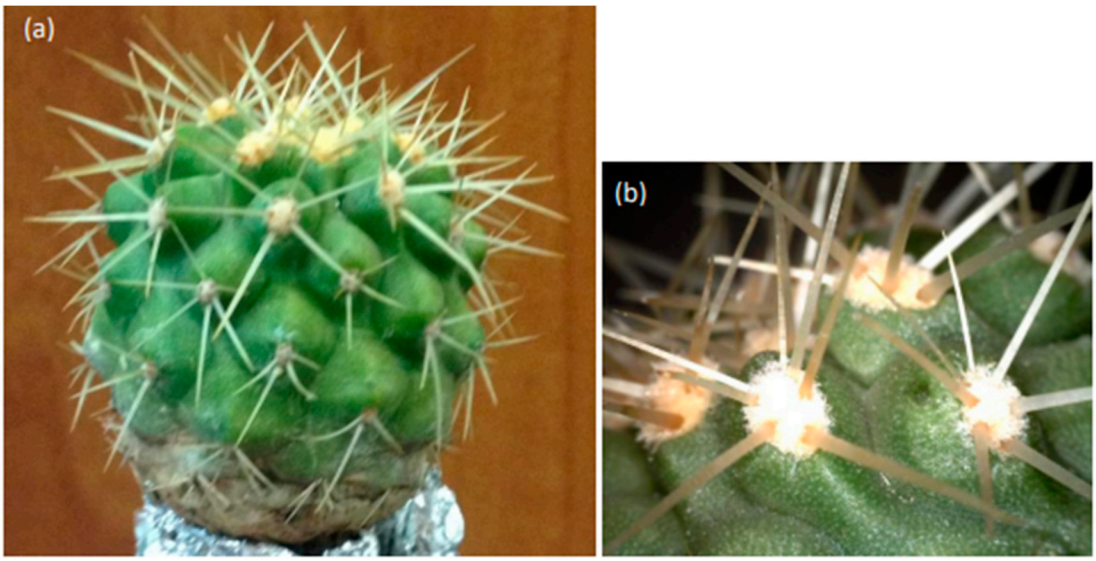

Figure 1. Photo of *Copiapoa cinerea* that was used to replicate the stem and spine microstructures—(**a**) whole plant, (**b**) close-up of the stems emanating from the areoles.

2.2. Fabricated Surface Design of C. cinerea

Utilizing the surface measurements of *C. cinerea* (the stem and spines), replicated surfaces of these macro-structures were designed for four different surfaces, namely a flat surface, a stem surface, a surface with an array of spines, and finally, a surface with a combination of both stem and spine features (Figure 2). A channel was also incorporated into the design to ensure that water run-off could be collected and not lost.

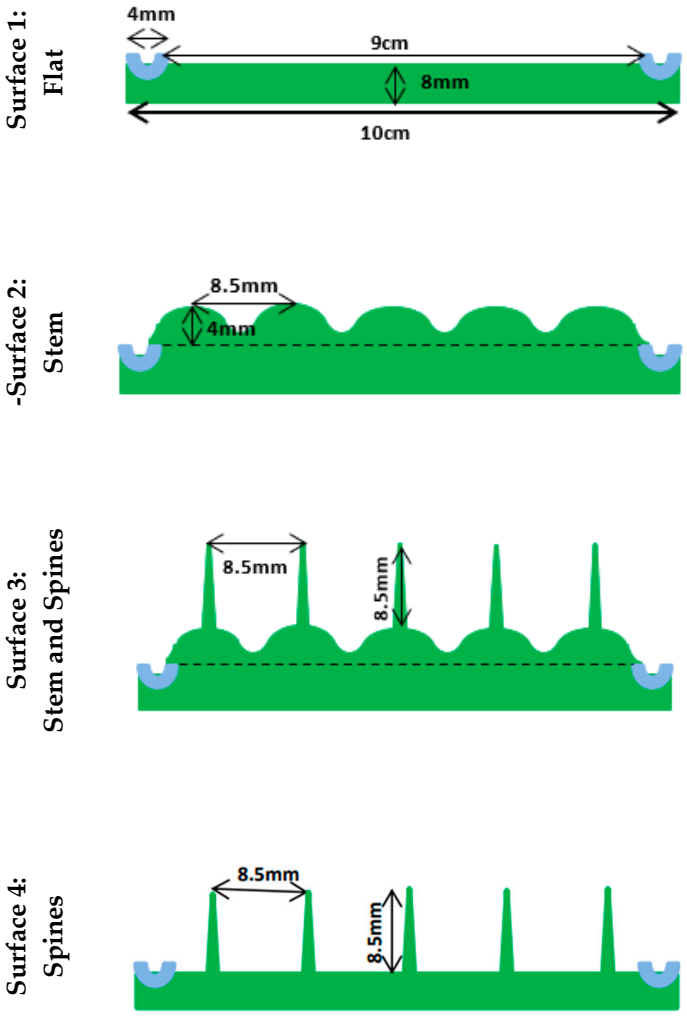

Flat inner square surface void of macro-structures (9 × 9 cm) with a surrounding channel (4 mm width) and an overall area of 10 × 10 cm. The depth of 8 mm for this flat surface is the same for the other replicated surfaces (not accounting for the height of the different macro geometrical shapes above the flat).

Using computer–aided design (CAD), nipples are sunk into holes cut in the flat metal plate to create a bumpy array of peaks and troughs, with a spacing of 8.5 mm apart from peak to peak to fabricate the stem features of *C. cinerea*.

Using CAD-designed stem features which were sunk into holes cut into the flat metal plate to create a bumpy array of peaks and troughs (i.e., sheet 2). Spine features obtained using metal needles sunk into holes drilled into the peak of each nipple and pointing vertically upright, each of a height 8.5 mm. A spacing of 8.5 mm apart from needle tip to needle tip.

On the flat metal sheet, spine features (8.5 mm height) are obtained using metal needles sunk into pre-drilled holes that are spaced 8.5 mm apart. The tips of each adjoining row of needles are aligned with the gap of the previous row and with every other row aligned.

Figure 2. Side-view design of four surfaces for fabrication of geometrical macro cacti features.

Due to the added complexity of the spine features, careful consideration was required to use a fabrication technique that could replicate both the stem and spine features of *C. cinerea*. Consequently, a mix of aluminium and steel was used, with aluminium being used for everything but the replicated spine features. The spines were constructed from steel.

Surface Fabrication Methodology of *C. cinerea*

Having designed the surfaces to be fabricated, a flat base structure (see Figure 3a) was made from aluminium for all four surfaces, each with a 4 mm wide surrounding channel. This ensured that all surfaces had the same footprint, with an approximate overall area of 100 cm^2. A channel to catch and direct surface water run-off was cut into the perimeter, leaving a 9 × 9 cm inner square surface on which the different replica shapes could then be added. The stem features (of dimensions shown in Figure 2, Surface 2) were first constructed using CAD (computer-aided design) SolidWorks software. These three-dimensional geometric stem shapes were then used by a milling machine that was programmed to follow the computer-aided design to cut the stem shape out of aluminium blocks. This method allowed for the consistency of each stem shape being machined.

Once all the stem shapes had been cut, holes were cut into the aluminium base structure (Figure 3a), and the milled aluminium stem features slotted into these pre-drilled holes (Figure 3b).

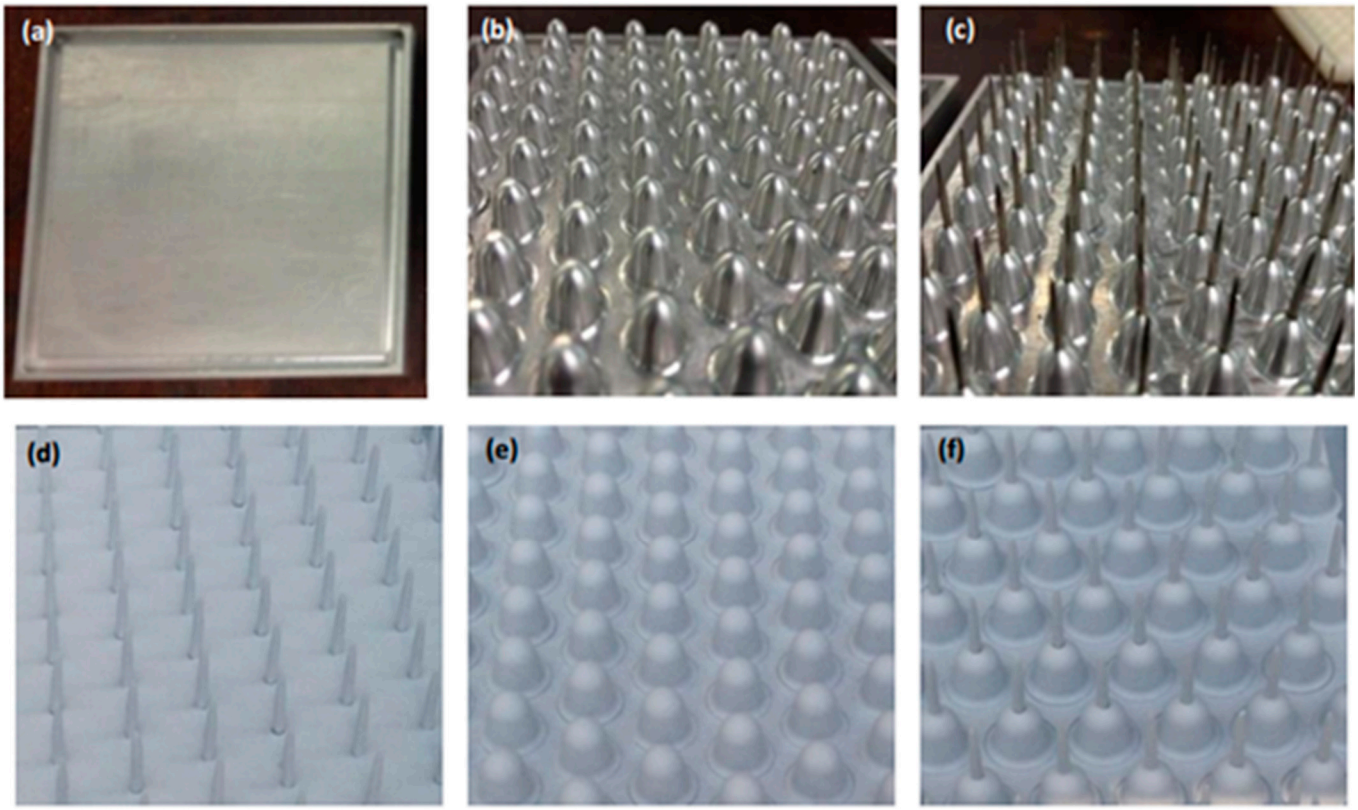

Figure 3. Replicated macro-structures before and after coating. Replicated surfaces: (**a**) uncoated aluminium flat surface with the drainage channel clearly visible around its perimeter; (**b**) uncoated aluminium stem replication; (**c**) uncoated aluminium stem with steel spine replication; (**d**) coated aluminium base with steel spine replication; (**e**) coated aluminium stem replication; (**f**) coated aluminium stem with steel spine replication.

In the same way, steel spines (with spine heights of 8.5 mm) were then machined to ensure that each were of equal length. These spines were then either individually slotted into pre-drilled holes on top of the stem features (Figure 3c) or, alternatively, slotted into the pre-drilled holes on one of the base plates (Figure 3d). To ensure that the dew-harvesting efficiency of these surfaces were maximized and to mitigate any inconsistencies that could occur from having a mix of steel and aluminium, all surfaces were coated with the same materials. Figure 3d–f show these coated surfaces. The coating consisted of five layers. The first was a white etch primer (that is designed for use on aluminium and steel surfaces and adheres to the plates) in preparation for the second layer, which was an undercoat, followed by a third top coating to protect them from the atmosphere. All four sheets then had two more top coatings of white paint mixed with the OPUR additive.

2.3. Harvesting, Collection, and Run-Off Efficiency Methodology

Three different methods were employed to evaluate the potential of the fabricated macro-surfaces as dew harvesters, using a climate chamber and outdoor conditions on dewy nights (Figure 4). These methods included the following:

1. Harvesting condensed water;
2. Collection of harvested condensed water;
3. Collection of run-off (30°) of condensed water.

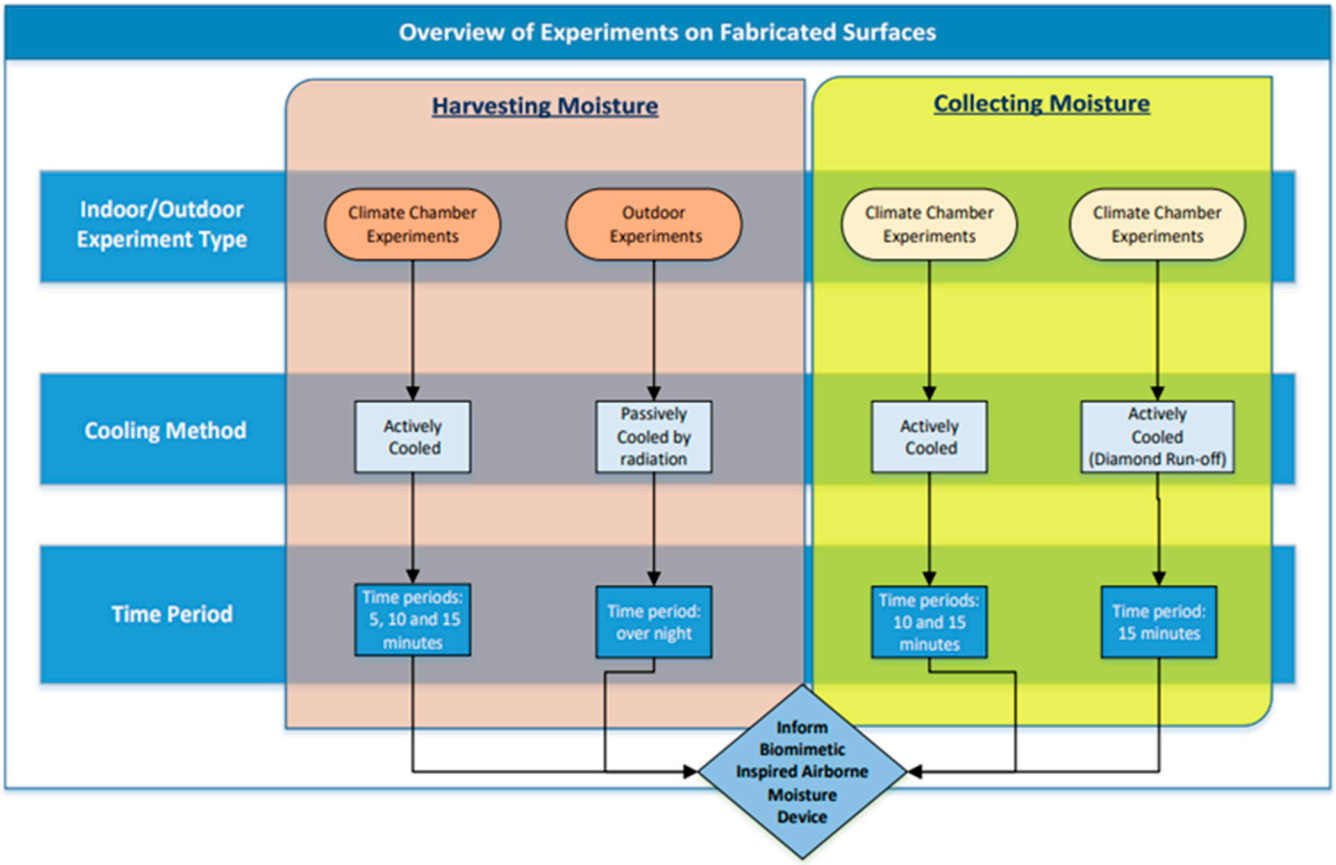

Figure 4. Overview of harvesting and collection experiments.

The first method involved measuring the harvesting efficiency of each replicated surface, followed by two different collection efficiency methods. The harvesting experiments were conducted for three different periods—5, 10, and 15 min—while the collection experiments were carried out over durations of 10 and 15 min. It is worth pointing out that, although the flat planar surface was used as the key reference material in this study, data were also collected for a Plexiglas surface to facilitate comparisons with past and future studies in this field. Plexiglas was chosen based on its use in a previous study for similar comparative reasons [18].

The flow path orientation was also analysed, comparing the diagonal surface water run-off with the parallel water run-off for a square orientated surface (see Figure 5). The square surface had two uppermost corners and two corners at the bottom, with a very slight incline to allow water to run into a collection pot along the lower channel. The diamond-orientated surface had one corner pointing vertically upward, with its diagonally opposite corner pointing vertically downwards and positioned above a collection pot.

Two different cooling techniques were used during this investigation phase, one active and the other passive (it should be noted that the passive experimental set-up in the climate chamber does not refer to the cooling mechanism). The passive cooling of the surfaces was simply radiative cooling from the night sky, and the active cooling utilized an ice pack to keep the surfaces cool. It should be noted that, while cooling a substrate using an ice pack cannot truly mimic radiative cooling with the night sky, actively cooling a substate is an effective alternative to test the surfaces under investigation in controlled environments. Actively cooling substrates for testing has been used effectively by other researchers assessing surfaces and droplet condensation effects and efficiency [25,26].

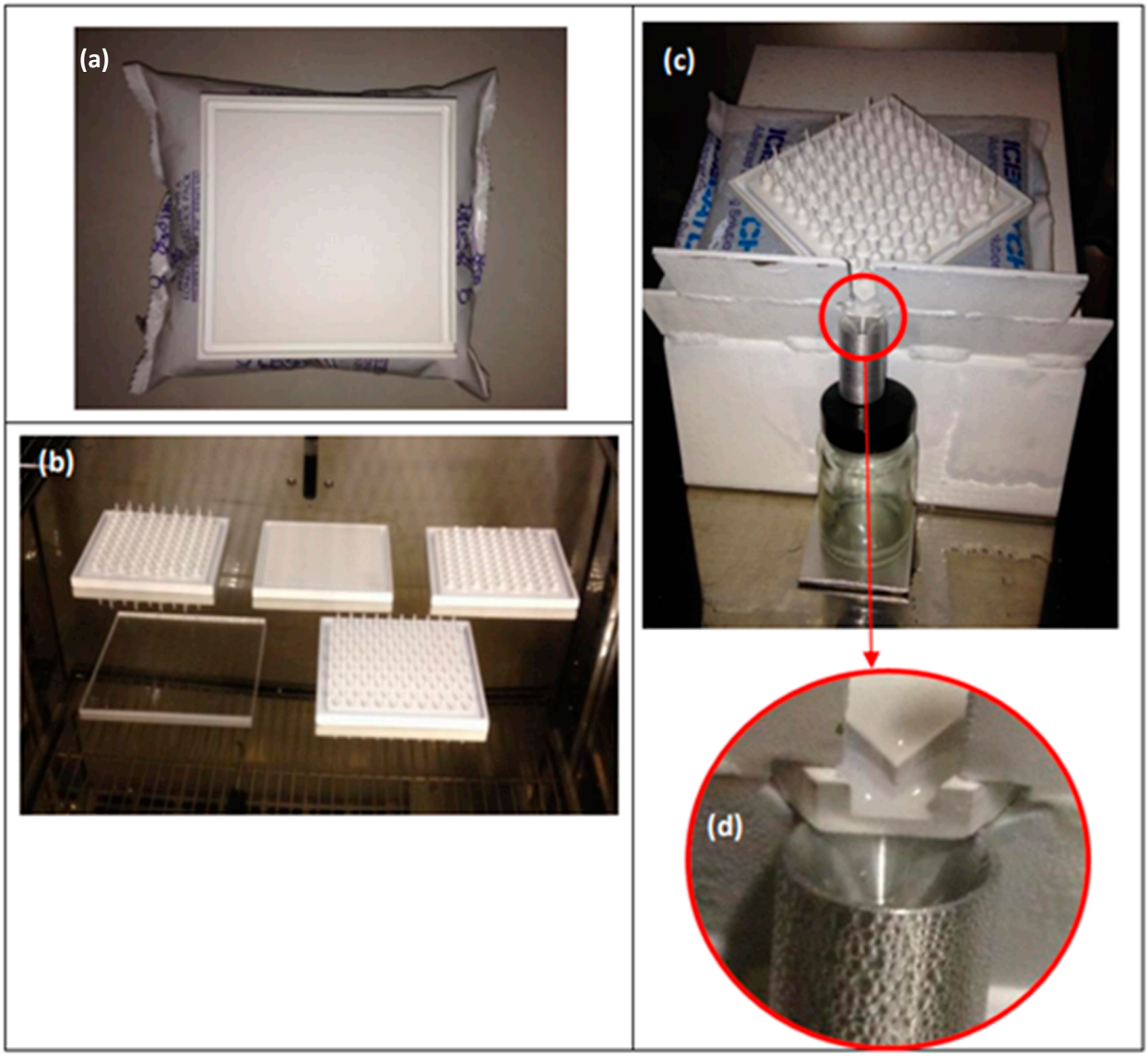

Figure 5. Experimental set-up in climate chamber for active and passive cooling of replica surfaces. (**a**) An example of an actively cooled horizontal surface on top of an ice pack; (**b**) passive surfaces (not cooled) and harvesting from flat/horizontal plane; (**c**) an example of one of the actively cooled surfaces, capturing run-off from surfaces that are inclined at an angle of 30° to the horizontal; (**d**) close-up of the draining point that is also seen in Figure 8 in the square verses diamond set-up.

Even though passive cooling is the main focus of this study, alongside the amount of dew water that condenses on the surfaces, active cooling was assessed to give an indication of what these replicated surfaces could collect if both a passive and active approach is taken. A percentage difference was subsequently calculated between how much water each surface could harvest or condense (either actively or passively in a horizontally flat position) with the amount of water collected from each surface over the same period. These data were normalized using the planographic surface area (i.e., the footprint of the surface) rather than the developed surface area, which is standard practice in dew harvesting [12,18]. Furthermore, as L/m^2 is what is typically used when reporting on atmospheric water harvesting (AWH) [22,27,28], this study has chosen to use this when reporting on the water collected so that others in the field can use these results for comparison.

2.3.1. Climate Chamber Experiments

The four different climate chamber experiments were all run at a relative humidity of 97% and at a temperature of 35 °C. As discussed above, three water capture experiments were run, namely harvesting condensed water, collecting the harvested condensed water, and finally the condensed water run-off (30°). This was followed by an experiment involving no active cooling (passive) of the replicated surfaces to assess their harvesting efficiency of condensed water under the same climatic conditions. An example of the set-up of the actively cooled and the passive experiments in the climate chamber are given in Figure 5.

For the cooled surfaces, the process involved two stages: firstly, placing the surfaces in a freezer for 1 h before transferring them to the climate chamber, and secondly, actively cooling them throughout their time in the climate chamber using a frozen ice pack. All ice packs used were non-toxic, of the same make, size, and gel type ("Icecatch Gel packs"), ensuring consistent surface cooling.

The freezer temperature was measured at −13.6 °C ± 1 °C using a handheld thermocouple. The ice pack, having been left overnight in the freezer, had a surface temperature of −12 °C ± 0.3 °C. After 15 min in the climate chamber, at the experimental settings of RH = 97% and a temperature of 35 °C, it recorded a surface temperature of −1.3 °C ± 0.4 °C (though its core temperature could have been different). The surface temperature of one of the replica surfaces was measured after 15 min in the climate chamber and was found to be approximately 26 °C. All experiments in the chamber were repeated ten times.

Both the harvesting and collection of condensed water were conducted on horizontal surfaces. In the first case, the harvesting data were measured by weighing each surface before and after the formation of surface condensation in the climate chamber for different periods (5, 10, and 15 min).

In the second experiment, the collection of the harvested condensed water involved placing the actively cooled surfaces into the climate chamber for different periods (10 and 15 min). Afterward, the surfaces were removed, and any surface water harvested was tipped onto the weighing scales (at no particular angle). It is important to note that this collection efficiency does not account for the amount of water harvested on the replicated surface area but rather focuses on the amount of run-off water collected (after harvesting from a horizontal position) and collecting this run-off water from the tilted surface.

The third set-up, the run-off of the condensed water, was conducted with each of the surfaces set at 30° to the horizontal, orientating the surface such that its diagonal corners were at the uppermost and lowest points (in a diamond-shaped configuration; see Figure 5c) with the lowest corner (or draining point, as shown in the close-up in Figure 5d) above a pot. This pot was used to collect the surface water run-off over the relevant period under investigation. The pot was weighed before and after to assess how much of the surface-condensed water had been collected. The incline angle of 30° was chosen, as studies had found that planar dew harvester efficiency increased by 35% when set at 30° from the horizontal [11,12].

2.3.2. Outdoor Experiments

After fabricating the macro features of *C. cinerea* on square plates of aluminium (including stem structures, stem with spines, standalone spines, and a smooth flat plate), and completing the climate chamber work, all three surfaces were placed outside on dewy nights (with the difference between the air temperature and dew point temperature on these nights always being less than 4 °C). The smooth, flat aluminium plate served as a reference, along with the Perspex sheet.

These surfaces were tested for their harvesting ability and were laid horizontally on top of a sheet of polystyrene foam for insulation, positioned on a flat roof that was visible to the night sky with no overhanging objects or buildings. This experiment was run over 10 different dewy nights in 2014 and 2015.

3. Results and Discussion

This is split into two sections. The first section covers the climate chamber results, specifically the harvesting experiments that were conducted along with the collection of surface water, and the second section focuses on the outdoor dew-harvesting experiments.

3.1. Climate Chamber Experiments

3.1.1. Harvesting Data

The primary data set for this experiment is presented in Figure 6. As mentioned earlier, harvesting experiments were conducted for three different time periods. For the actively cooled surfaces, three time periods were used: 5, 10, and 15 min. However, for the passive surfaces, data were acquired over a 10 min time period only. This decision was based on the observation that, as expected, minimal surface condensation occurred for the passive replica surfaces within the 10 min timeframe in the climate chamber (Figure 6a) when compared with the actively cooled surfaces. Hence, for the purpose of performance comparison, capturing additional passive data was deemed unnecessary.

The actively cooled stem & spine replica was identified as the most efficient in harvesting surface water when compared to the other surfaces under examination (when the data were normalized to the footprint surface area (Figure 6a), across all three time periods. Moreover, when comparing the three replicated surfaces, namely the stem, stem & spine, and spine only, to the flat reference surface, they exhibited statistically higher efficiency in water harvesting.

It was deemed important to also assess the data when normalized to the topographic surface area for these initial climate chamber experiments, as the cooling mechanism in the chamber (i.e., that of heat transfer via convection) was different from that of outdoor nocturnal radiative cooling of surfaces with the night sky. Thus, topographic data become important in this case as the surface is cooled, not just that which is visible from above (i.e., the footprint), which means that condensing water droplets form on the entire surface that is cooled.

With this in mind, the footprint data were normalized to the topographic surface area for each of the replica surfaces (Figure 6b). It was found that the spine replica is marginally more efficient than the other replica surfaces for all three time periods, and the three replicated surfaces were statistically more efficient at harvesting water when compared to the flat reference surface. It is known that the conical nature of spine features produces a Laplace pressure gradient that effectively drives droplets from regions of smaller radii (top of spines) to those of larger radii (bases of spines), with the droplets exhibiting a contact angle hysteresis [16,29]. It is thought that this could explain the spine replica's increased efficiency, effectively being able to move water droplets down the spines and making space for further condensation.

The data clearly indicate an increase in the amount of condensed water harvested on each surface the longer the actively cooled surface was kept in the chamber. After 5 min, the spine replica marginally outperforms the other surfaces in terms of water harvested, but the performance levels with the stem & spine replica after 10 min. However, it becomes notably more efficient compared to other surfaces after 15 min.

Interpreting normalized data does, however, require caution, as the topographic area does not necessarily contribute to the dew-harvested surface area. However, normalizing the initial climate chamber results to both the footprint and topographic surfaces was crucial to assess the potential condensation on the entire surface, not just the footprint regions. Since footprint data are vital to any dew-harvesting study, the subsequent climate chamber experiments focused exclusively on these replica surfaces at one of the three time periods used. Therefore, all data from here on are normalized to the footprint, a method traditionally considered the most appropriate in the field of dew harvesting.

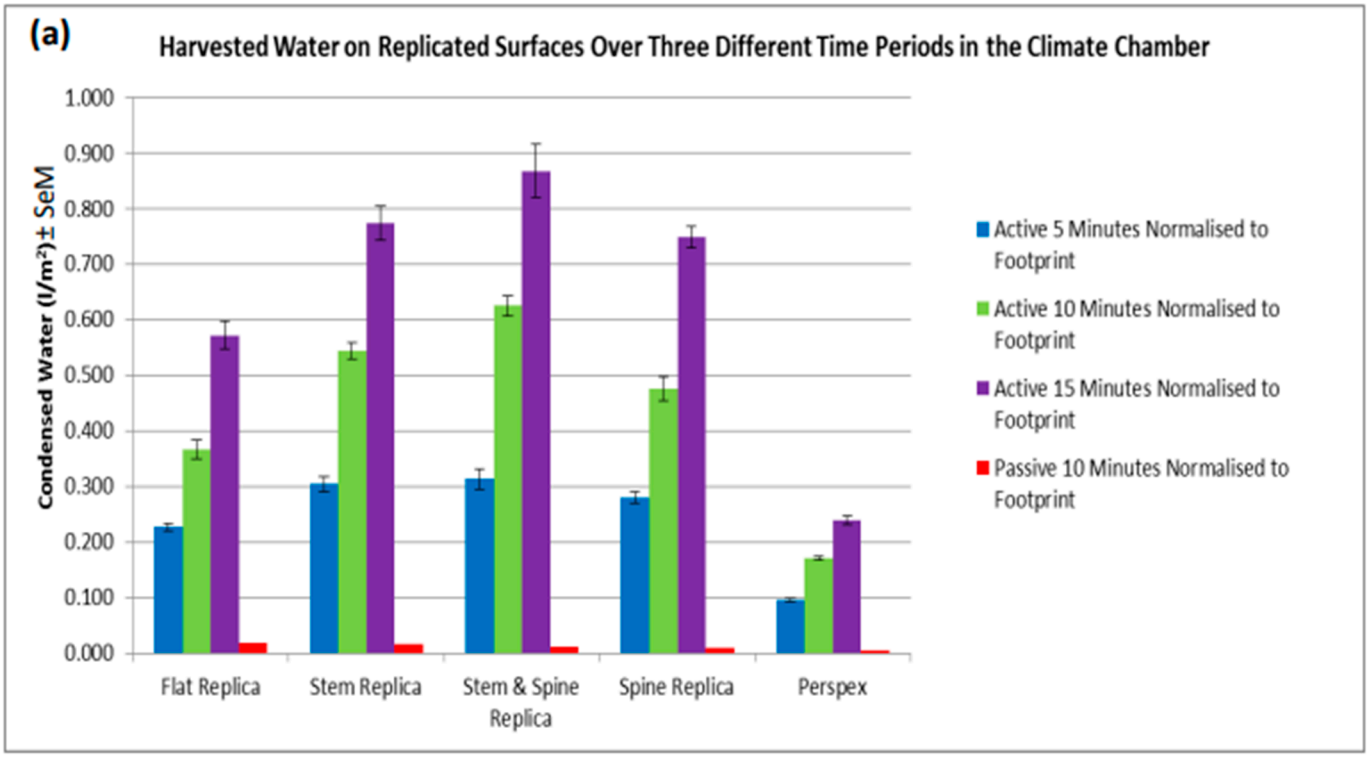

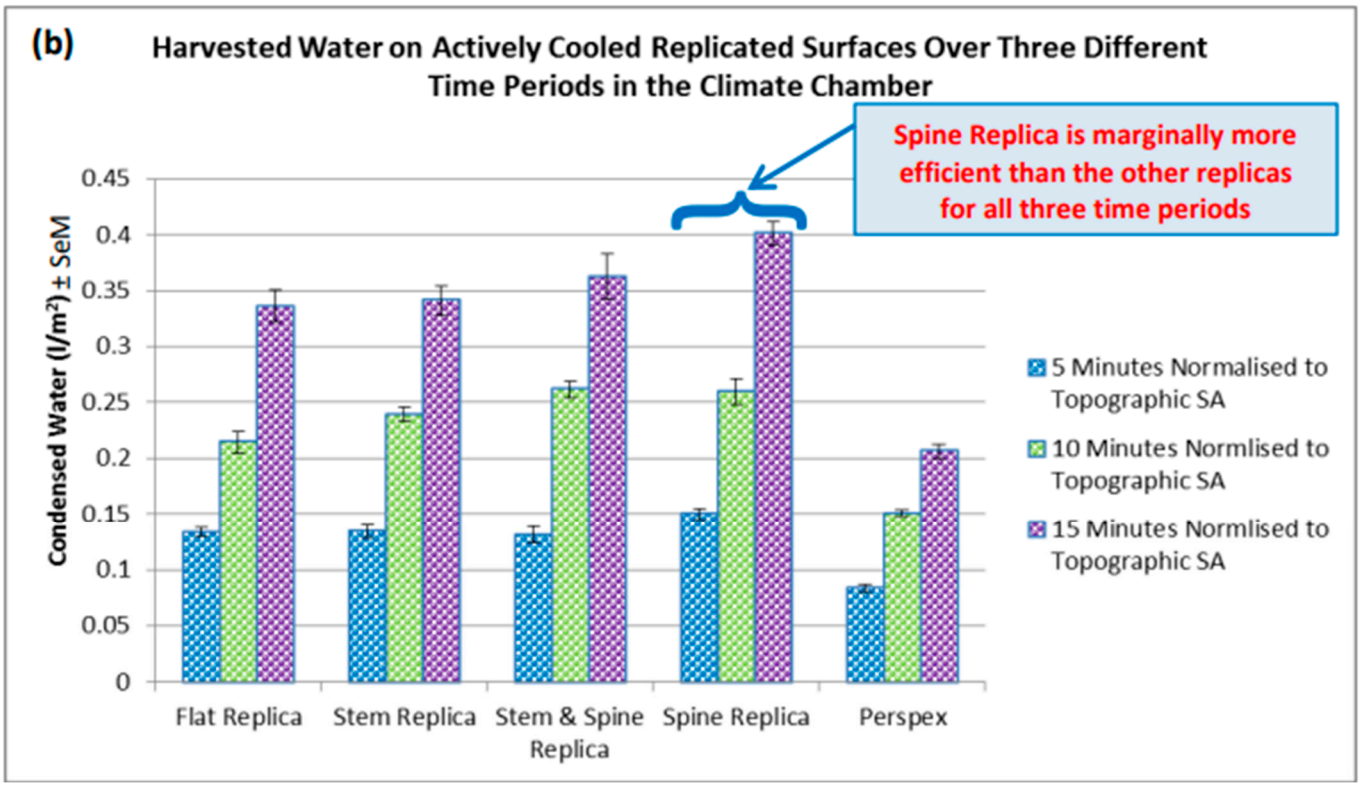

Figure 6. Harvesting climate chamber results for three different time periods. The results illustrated are shown for two different surface area normalizations: (**a**) actively cooled and passive data normalized to footprint (planographic); (**b**) actively cooled data normalized to topographic surface area.

3.1.2. Collection

Using the same set-up as in the harvesting experiment, discussed in the previous section, at the end of each time period (in this case, 10 min and 15 min), the surface-condensed water was tipped off each individual surface and measured. It is clear from Figure 7 that more water was collected for each of the surfaces after 15 min than after 10 min, with the stem & spine replica along with the stem replica collecting marginally more than the other replica surfaces. When comparing the stem replica, the stem and spine replica, and the spine replica with the flat reference surface, they are all significantly more efficient at collecting water.

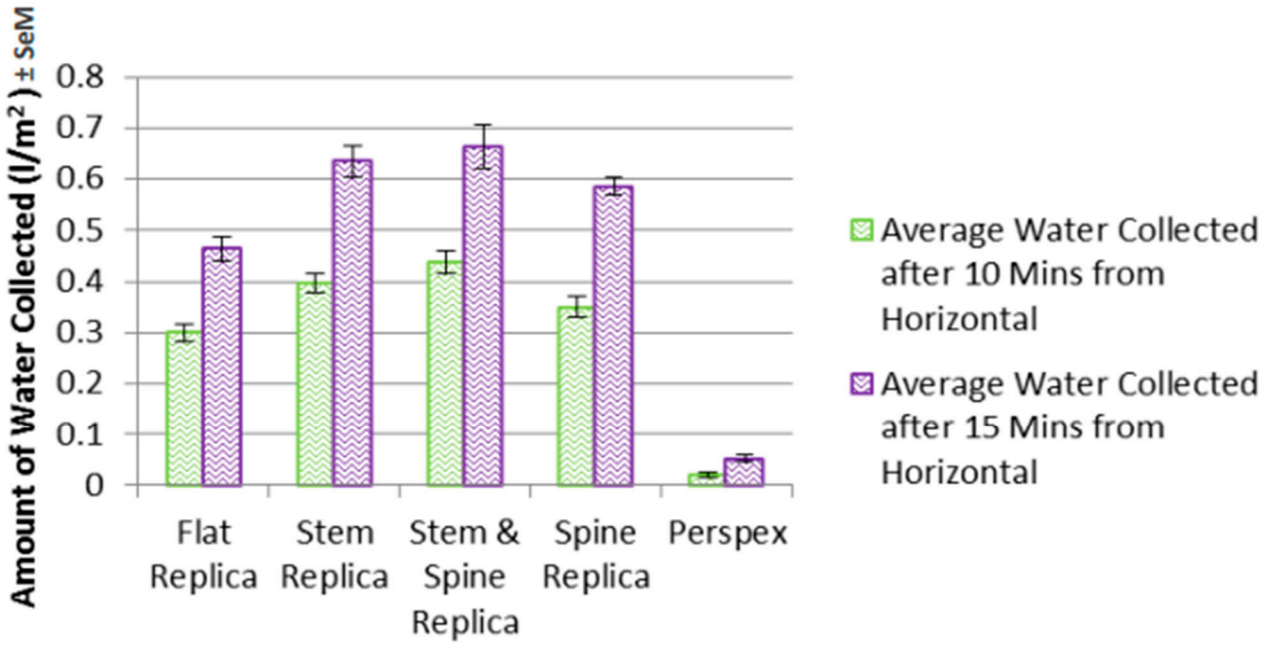

Figure 7. Collection results for two different time periods in a climate chamber.

Analysing these data in comparison with the average amount of water that was harvested (i.e., the average amount of surface water condensed on each surface), it was found that each surface only managed to collect a certain percentage of the harvested water (the data for this are given in Table 1). Thus, some water remains pinned to the surface and not collected, which could be due to the nature of the surface, possibly the paint or the additive in the paint that, whilst it encourages dew to harvest, it may hinder efficient surface water run-off and is something that would need further exploration in the future. After 15 min, the stem replica is the most efficient at collecting the most amount of surface water compared to the other surfaces and time periods. However, the flat replica had an edge over the other surfaces, consistently (over both time periods) collecting over 80% of the surface water harvested.

Table 1. Collection versus harvested condensed water.

Percentage (%) of Collected Water Compared with Harvested Water		
	10 min	**15 min**
Flat Replica	81.83	81.20
Stem Replica	72.91	82.12
Stem & Spine Replica	69.95	76.58
Spine Replica	73.41	78.17
Perspex	11.92	21.67

In a study by Park et al. [30], surfaces were fabricated to investigate droplet growth and movement by combining surface structures inspired by bumps on the Namib Desert beetle, a cactus spine (asymmetric channel based on a cone-like structure), and a pitcher plant's smooth (on a molecular level) surface. These researchers observed that the droplet growth increased due to an enhanced diffusion flux at the apex of the beetle-like bumps, comparable to those found on the cactus (as stem features) in this research. These droplets were then transported directionally along a molecularly smooth surface, mimicking the functional ability of cactus spines' asymmetric channel. This directional movement of surface water was also identified on the spines of *C. cinerea* [19] and acknowledged by others in the field [16,31], which underscores the importance of considering not only the harvesting but also the collection of airborne moisture in the design of dew-harvesting systems.

3.1.3. Run-Off

During the collection of surface water when the water was tipped off each surface by hand onto the scales, it was observed that there appeared to be a better run-off when the surface was positioned in a diamond shape rather than square. As such, it was decided that, before gathering data over different time periods to assess run-off collection efficiency, the square and diamond orientation of surfaces should be measured to see if there was any difference in their run-off harvesting efficiency.

Square Verses Diamond Run-Off of Water

This particular climate chamber experiment was deemed essential before running outdoor experiments, comparing the square verses diamond orientation efficiency collection of run-off surface water. The reasoning behind this was to explore the effect of flow path tortuosity on collection, along with assessing what impact edge effect orientation could have on the amount of water collected. Two surfaces were chosen to study the orientation efficiency: the flat replica and the stem replica. Two stands were built (one for the square orientation of replicas and the other for the diamond orientation) to hold the replica surfaces at an angle of 30° to the horizontal, regardless of orientation, along with the ice pack to enable the surfaces to be actively cooled for the required time. Both stands were placed in the climate chamber simultaneously to assess both orientations of the same surface structure side by side in exactly the same conditions (Figure 8).

The square-orientated surfaces were angled very slightly to facilitate the run-off of water into the surrounding channel to be directed into the collection pot below. However, this set-up presented some initial challenges. Firstly, it was observed that if the square-orientated replica was not positioned correctly, water would run down the surface and accumulate in the channel at the bottom without flowing into the collecting pot. Secondly, water run-off from the diamond-orientated surface was observed to be drawn backwards as it dripped off the replica's corner into the pot, often missing the pot entirely. This issue was addressed by positioning the collecting pot in direct contact with the edge of the replica's corner (i.e., no gap), ensuring that the run-off water flowed directly into the pot. A third challenge arose due to the presence of two stands in the chamber. Vibrations in the chamber caused the colleting pots to move. To counter this, L-shaped pieces of metal were introduced to stabilize the pots and prevent any unwanted movement. Additionally, the chamber's vibrations, combined with water pooling around the bottom of each stand, occasionally caused the stands to shift. This was resolved by placing absorbent paper sheets under the stands.

Having ensured a stable and consistent set-up, data were collected for the stem replica that was orientated in both a square and diamond set-up, over a 15 min period, with each experiment repeated ten times. In the same way, data were subsequently collected for the flat replica for both orientations. The collection pot was weighed (without its top) before being placed into the chamber and again after 15 min (with any condensation on its outer surface wiped dry).

Figure 8. Actively cooled square verses diamond set-up for 30° run-off.

The data gathered show that for both the stem replica and the flat replica surface, the diamond orientation is more efficient at collecting run-off surface water. In the case of the flat replica, it is approximately 34% more efficient, and for the stem replica, it is about 41% more efficient (Figure 9). This increased efficiency in the diamond configuration is believed to be due to edge effects, effectively doubling compared with the flat configuration. The significance of edge effects has been discussed in detail by Medici et al. [25]. Droplets condensing on or near such geometric discontinuities can receive more vapour (especially at the corners or edges), leading to a faster droplet growth potential. As the droplets become larger, they tend to become unpinned from the surface and run down it, carrying other droplets in their path. This clearing effect makes more space for additional water to condense.

It can be seen in Figure 9 that the level of collected surface water (L/m^2) from the different surfaces are distinct with small error bars. There is a clear trend between the surface water collected when the surface under investigation is orientated in a square manner compared to when the same surface is placed in the diamond orientation. Figure 9 illustrates the notable increase in the efficiency of collected water for the diamond configuration for both a flat surface and the stem replica surface. For this reason, the remining run-off experiments in this study used the diamond orientation set-up.

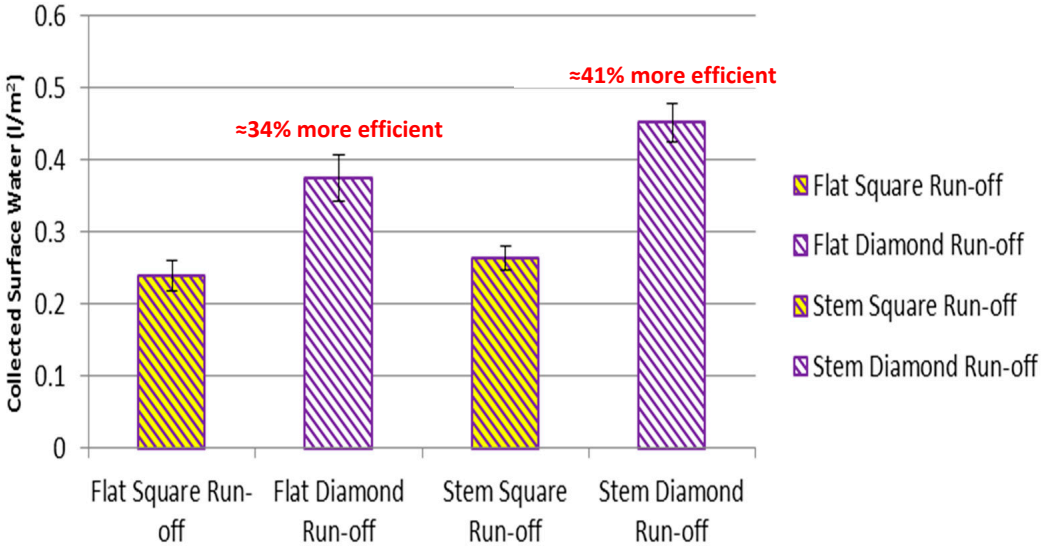

Figure 9. Comparative water run-off results for diamond- and square-orientated surfaces after 15 min in a climate chamber.

Diamond Run-Off (30° to the Horizontal) of Water

After determining that the diamond orientation was the most effective for collecting the surface-condensed water run-off, all the replica surfaces were tested in the climate chamber over a 15 min period, arranged in the diamond run-off configuration. The same stand was used from the previous experiment, with the same set-up but without absorbent paper under the stand. This adjustment reduced water pooling, as there was only one melting ice pack, ensuring that the stand remained stationary throughout. Additionally, this set-up facilitated the easy drainage of any water under or around the stand every 15 min, in between placing the next replica surface under investigation into the chamber.

Upon comparing the data for the flat replica and stem replica with the diamond orientation data from the previous section, it is noticeable that the average amount of water in this instance is slightly less. This outcome was expected because there was less moisture content in the chamber, attributed to having only one ice pack (compared to two in the previous experiment). Moreover, there was no need for absorbent paper under the stand, resulting in less water pooling near each replica under investigation. This reduction in pooled water could, in turn, decrease the amount of water available to condense on the replica surfaces. However, due to the substantial variability in these data (Figure 10a), no statistical significance could be established.

It is interesting to see, however, the condensed water droplets that formed on the different surfaces under investigation, as shown in Figure 10b–e. The edge effects of the spine feature were clearly demonstrated with the droplets along these spines, something that Medici et al. [25] found to be due to the additional water vapour surrounding discontinuities, which enhances droplet growth. The condensed droplets on the flat surface seen in Figure 10c do not have droplets as large as can be seen on the other fabricated surfaces. Whilst this study did not analyse the droplet distribution and nucleation sites over time on the surfaces, this is something that could be explored in the future, in a similar manner as outlined by Baghel et al. [32].

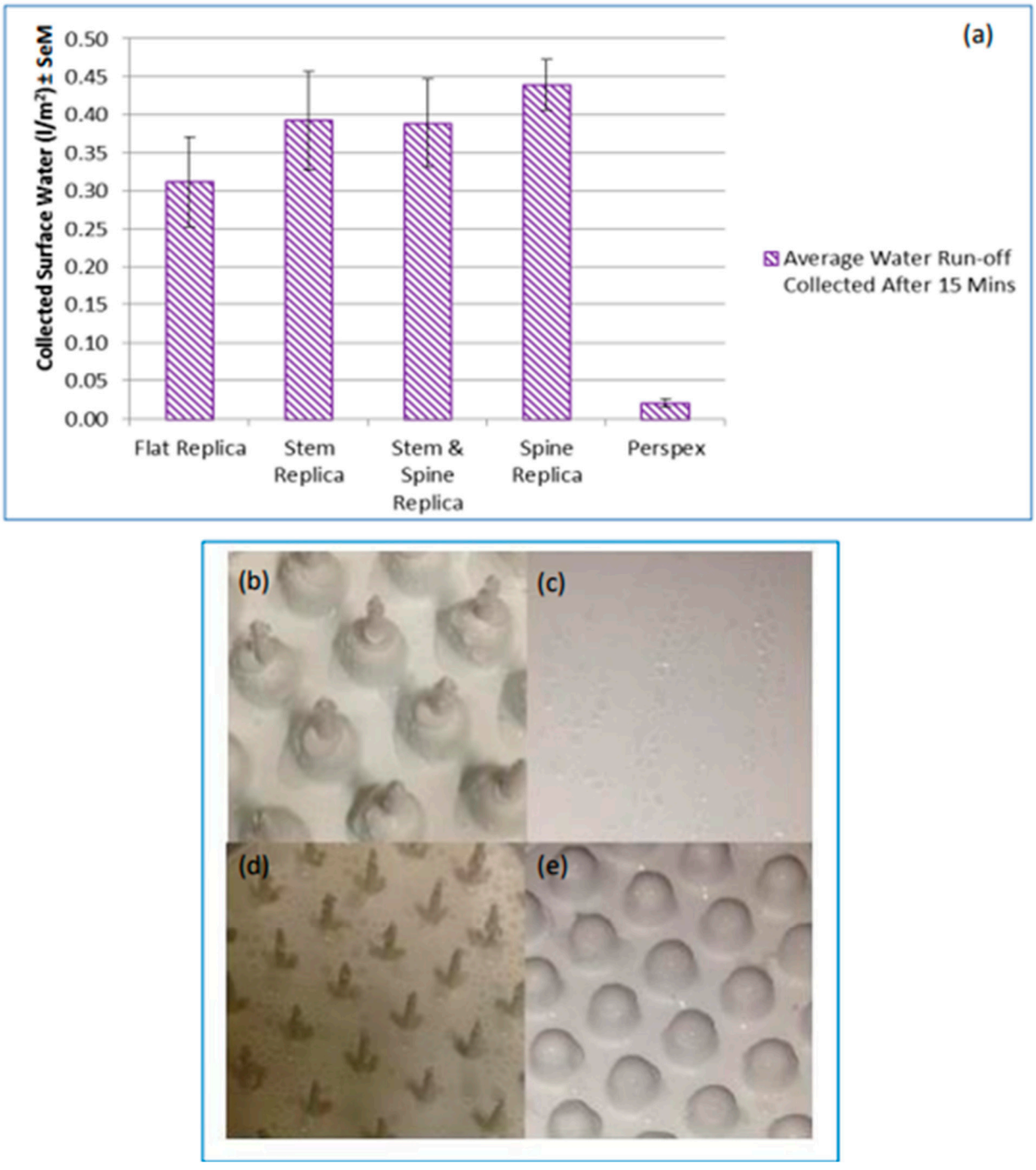

Figure 10. (**a**) Amount of water run-off at 30° to horizontal in climate chamber over 15 min; (**b**–**e**) photos of condensed droplets on the surfaces under investigation.

3.1.4. Comparison of 15 Min Data

Taking the three different sets of data, namely horizontal harvesting, surface collection (following horizontal harvesting), and 30° run-off, all over the 15 min time period, a graph was drawn up to compare the data from the climate chamber experiments (Figure 11). It is clear that the amount of water collected from the flat surface at 15 min is not only more than the amount of surface water collected (by tipping the replica surfaces after water had condensed on the horizontally positioned surface) over the same duration, but also more than when compared with angling each surface at 30° to the horizontal and measuring the water run-off over the duration of 15 min.

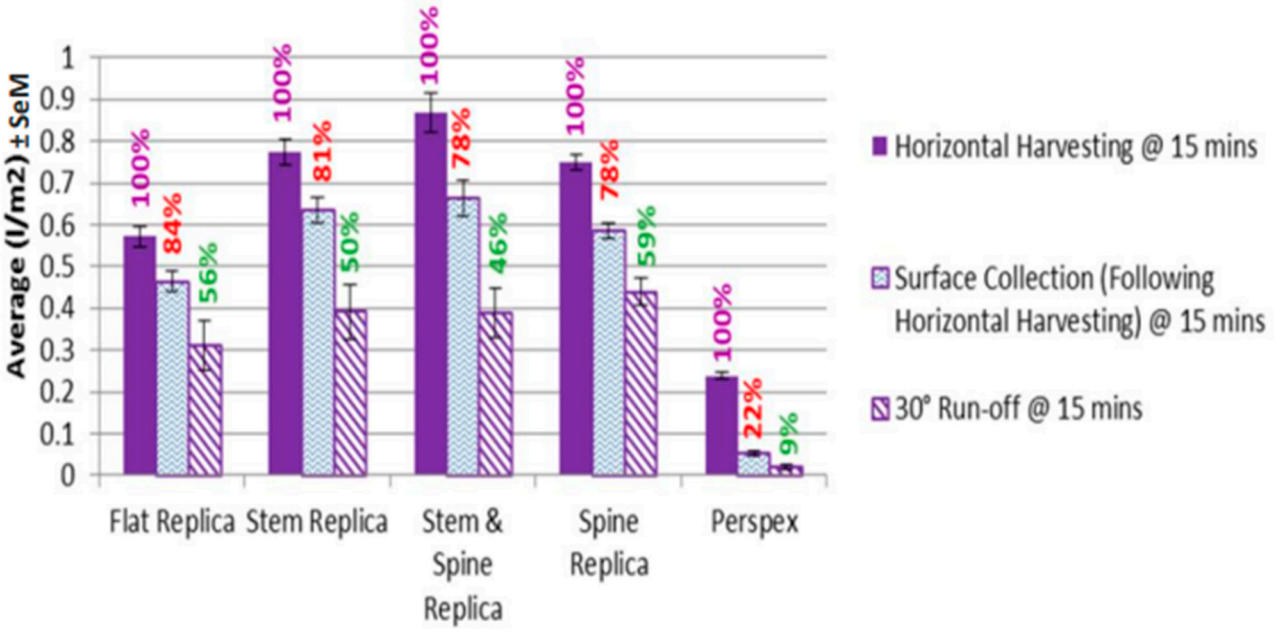

Figure 11. Comparative 15 min climate chamber data for three different water-collecting methods. Showing the average amount of water that was harvested (from horizontal), collected (from horizontal), and the 30° run-off, all over a 15 min time period.

The present findings suggest that, in practical dew-harvesting scenarios, laying the harvesting surface horizontally and then tipping off the surface water at the end of the dewy night, before it evaporates in the sun, may be more efficient than keeping it inclined for the entire night. This efficiency is likely attributed to the evaporation process on inclined surfaces, where surface water is spread out and may not have sufficient time to accumulate and then run off the surface effectively. In contrast, on horizontal surfaces, condensed water builds up over time. When the surface is then tipped to drain, there are larger droplets of water that take more of the accumulated surface water with them as they roll off into a collector. This process enhances the overall efficiency of the dew-harvesting system.

Statistically, it was found that this effect held for all the replicas when comparing the three different methods of collecting surface-condensed water:

1. Flat Replica: there is an effect of the collection method ($p < 0.0007$). Harvesting was more efficient than the collection ($p < 0.0008$), and the collection was more efficient than the run-off ($p < 0.0143$);
2. Stem Replica: there is an effect of the collection method ($p < 6.7e\text{-}6$). Harvesting was more efficient than the collection ($p < 1.8065e\text{-}07$), and the collection was more efficient than the run-off ($p < 0.0047$);
3. Stem & Spine Replica: there is an effect of the collection method ($p < 3.16e\text{-}6$). Harvesting was more efficient than the collection ($p < 2.88e\text{-}05$), and the collection was more efficient than the run-off ($p < 0.0038$);
4. Spine Replica: there is an effect of the collection method ($p < 5.6423e\text{-}09$). Harvesting was more efficient than the collection ($p < 5.6569e\text{-}10$), and the collection was more efficient than the run-off ($p < 0.0018$);
5. Perspex: there is an effect of the collection method ($p < 1.61e\text{-}19$). Harvesting was more efficient than the collection ($p < 3.07e\text{-}8$), and collection was more efficient than the run-off ($p < 0.0051$).

3.2. Outdoor Macro Replicated Results and Discussion

With the main outdoor experiment measuring the amount of dew water harvested on the fabricated surfaces from a horizontal position, the amount of dew that had formed on the surfaces was measured (Figure 12). It was found, over the 10 dewy nights, that

the replicated macro-surface that harvested, on average, the most amount of dew was the stem with spines replica, with 0.174 L/m^2 ± 0.016 L/m^2 of dew harvested (± the standard error of the mean). This was followed by the spine, the stem, and, finally, the flat replica with average dew harvests of 0.173 L/m^2 ± 0.015 L/m^2, 0.171 L/m^2 ± 0.017 L/m^2, and 0.164 L/m^2 ± 0.015 L/m^2, respectively. These data are illustrated in Figure 12a with the blue bar chart.

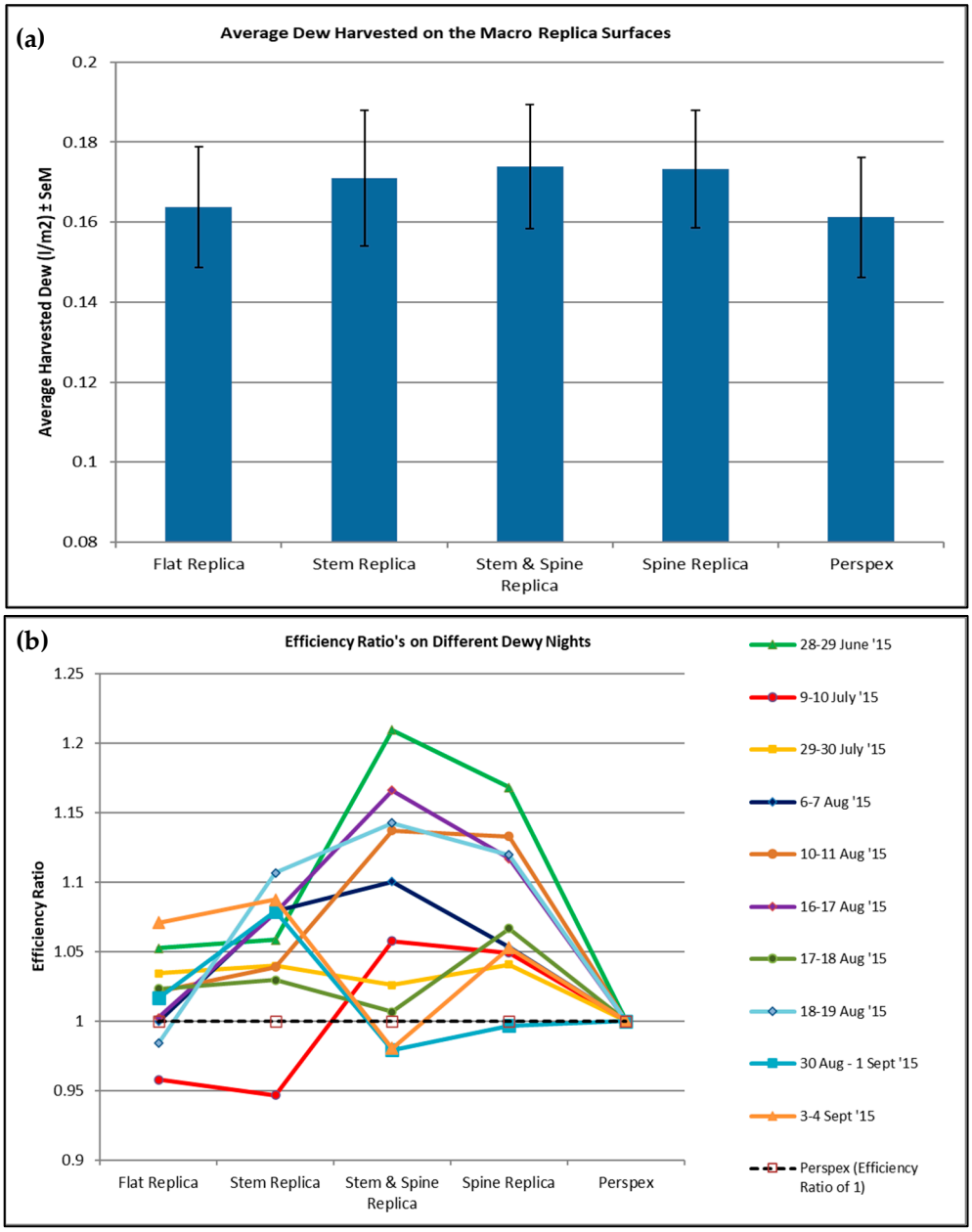

Figure 12. Dew-harvesting data of replicated macro-surfaces: (**a**) graph illustrating the average dew in L/m^2 ± SeM for the replica surfaces; (**b**) graph illustrating the efficiency ratio of the replica surfaces over different dewy nights compared with the Perspex control.

Each night of data collection was also plotted to assess the trend of efficiency compared against the Perspex sheet (i.e., the line graphs in Figure 12b). Hence, the Perspex always had an efficiency ratio (E_R) of 1. The stem & spine replica had the highest average efficiency ratio of 1.081 ± 0.026, followed by the spine replica, the stem replica, and finally the flat replica, with average efficiency ratios of 1.080 ± 0.017, 1.054 ± 0.014, and 1.016 ± 0.010, respectively. Looking at the data set for each of the dewy nights recorded, the flat replica

had a lower efficiency ratio than the Perspex on three of the recorded nights and the stem & spine replica on two nights, and the stem recorded one E_R lower than the Perspex, as did the spine replica.

Statistically, compared to the Perspex, these data are significant for the stem & spine replica, the spine replica, and the stem replica, with *p*-values of <0.0061, <0.0001, and <0.0013, respectively. Thus, the spine & stem replica, the spine replica, and the stem replica show a significantly increased efficiency ratio of harvested dew water over the recorded ten nights. The efficiency ratio data over the recorded dewy nights have also been plotted (Figure 13).

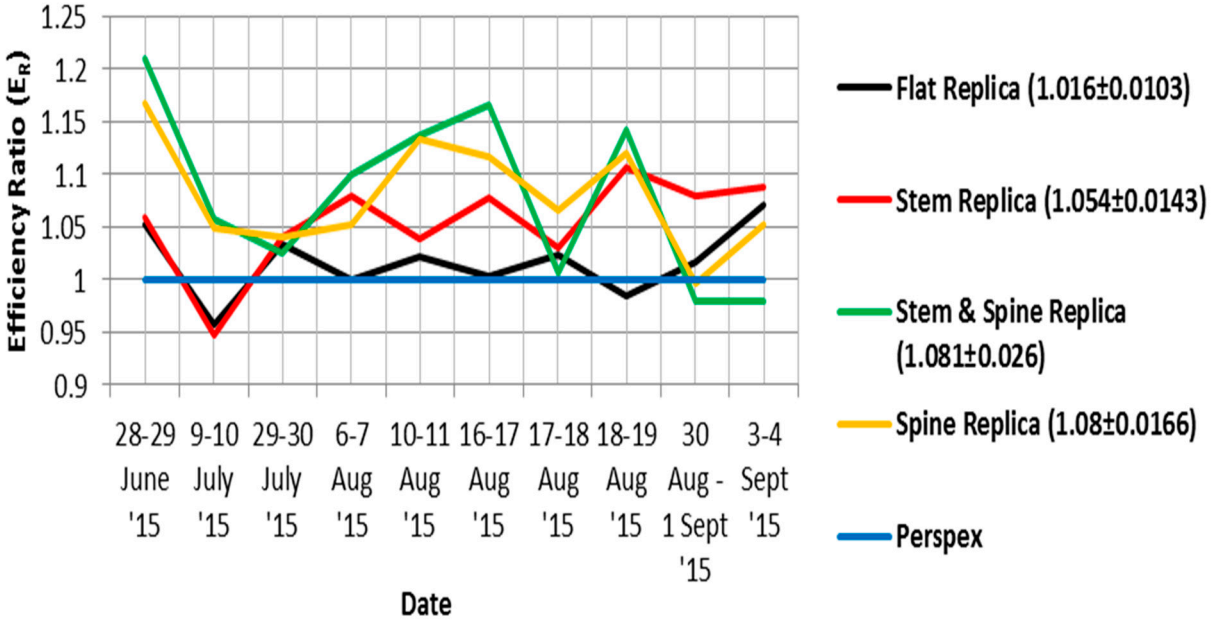

Figure 13. A plot of the dew-harvesting efficiency ratio data (mean ± SeM) for the different surfaces under investigation.

The reason for the observed increased efficiency ratio remains unclear, and further experiments are needed to gain a better understanding. Nonetheless, Beysens et al. [22] demonstrated that surface geometry significantly influences the amount of dew harvested. Their study found that origami and egg-box dew harvesters were more effective than a flat surface devoid of macro-structures. They suggest that the flow of dew with evaporation on the flat peaks of the egg-box shapes limited dew growth due to evaporation and a lack of flow. Applying this reasoning, the spine and stem geometry used in this study could potentially increase the flow of dew along their sides, providing free nucleation points for dew to form.

Contrastingly, a study by Kidron [33] found that a smooth Plexiglas surface was more efficient as a dew harvester than a "ragged Plexiglas" surface. This efficiency was attributed to potential variations in the radiative cooling efficiency, with the depressions on the rugged surface being less efficient in this regard. The OPUR additive used in this study addresses this concern by ensuring a uniform high IR emissivity across the entire coated surface. Additionally, the coating covers any microscopic irregularities on the surfaces, ensuring equal hydrophilic wetting properties across the surface. This aspect may have played a role in the differences found between the smooth and textured Plexiglas in Kidron's study.

In conclusion, this study compared each of the replicated surfaces, ensuring equality in terms of surface wettability and IR emissivity, to draw conclusions on the investigated structures. The results indicate that these biomimetic-inspired geometrical macro-structures enhance dew-harvesting performance, aligning with the findings of Beysens et al. [22].

4. Conclusions

Having measured the macro features of *C. cinerea* and fabricated surfaces based on these measurements, it was observed that both the spines and the presence of stem structures increased the dew-harvesting efficiency. Consequently, when replicating the stem and spine geometry and combining them on the surface, it was found to harvest an average of 0.174 $L/m^2 \pm 0.016$ L/m^2 of dew. This was compared to 0.164 $L/m^2 \pm 0.015$ L/m^2 for the flat reference surface and 0.173 $L/m^2 \pm 0.015$ L/m^2 for the surface with spine features.

However, it was noted that a percentage of the harvested surface water did not run-off; instead, it remained pinned to the surface. The range of collected surface water from these harvesting surfaces varied between 46% and 59% for the three different replicated surfaces. This highlights the importance of addressing water run-off issues in future studies to ensure that no harvested dew on the surface of a condenser is lost to evaporation and inadequate run-off into a collector.

These results are crucial to consider when designing a dew harvester, aiming to implement the best configuration to maximize harvesting and collection potential.

Such optimization could lead to significant improvements in airborne moisture harvesting, addressing the challenges posed due to climate change. In light of this, this research recommends the next step in fabrication and testing to assess the impact of microstructures similar to those found on the living cacti spines of *C. cinerea* on water run-off and collection when engineered and incorporated into the design of the fabricated macro-surfaces tested in this study.

Author Contributions: Conceptualization, T.M.; methodology, T.M., A.P. and D.G.; software, T.M. and D.G.; validation, T.M., A.P., D.G., F.B. and G.D.; formal analysis, T.M. and F.B.; investigation, T.M.; resources, D.G. and G.D.; data curation, T.M. and F.B.; writing—original draft preparation, T.M.; writing—review and editing, T.M., A.P., D.G., F.B. and G.D.; visualization, T.M.; supervision, A.P. and D.G.; funding acquisition, G.D and D.G. All authors have read and agreed to the published version of the manuscript.

Funding: This research was funded by Fujitsu and supported by HPC Wales and Swansea University. No grant details are available.

Informed Consent Statement: Not applicable.

Data Availability Statement: This formed part of a wider study that has the data included as part of the submitted PhD thesis [21].

Acknowledgments: This research paper was funded by Fujitsu and supported by HPC Wales and Swansea University. We thank ASTUTE for the use of their expertise with regard to scanning and geometric reconstruction for cacti component fabrication. We also thank OPUR (International Organization for Dew Utilization) for use of their alumina–silicate additive.

Conflicts of Interest: The authors declare no conflict of interest.

References

1. WHO. *Global Water Supply and Sanitation Assessment 2000 Report*; World Health Organization: Geneva, Switzerland, 2000; p. 9.
2. Gleick, P.H.; Iwra, M. Basic Water Requirements for Human Activities: Meeting Basic Needs. *Water Int.* **1996**, *21*, 83–92. [CrossRef]
3. Shiklomanov, I.A. World water resources. In *Water in Crisis*; Oxford University Press: New York, NY, USA, 1993.
4. Cook, E.R.; Woodhouse, C.A.; Eakin, C.M.; Meko, D.M.; Stahle, D.W. Long-term aridity changes in the western United States. *Science* **2004**, *306*, 1015–1018. [CrossRef] [PubMed]
5. Hiatt, C.; Fernandez, D.; Potter, C. Measurements of fog water deposition on the California Central Coast. *Atmos. Clim. Sci.* **2012**, *2*, 525. [CrossRef]
6. Tomaszkiewicz, M.; Abou Najm, M.; Beysens, D.; Alameddine, I.; Zeid, E.B.; El-Fadel, M. Projected climate change impacts upon dew yield in the Mediterranean basin. *Sci. Total Environ.* **2016**, *566*, 1339–1348. [CrossRef] [PubMed]
7. Muselli, M.; Lekouch, I.; Beysens, D. Physical and Chemical Characteristics of Dew and Rain in North-West Africa with Focus on Morocco: Mapping Past and Future Evolution (2005–2100). *Atmosphere* **2022**, *13*, 1974. [CrossRef]
8. Liu, X.; Beysens, D.; Bourouina, T. Water harvesting from air: Current passive approaches and outlook. *ACS Mater. Lett.* **2022**, *4*, 1003–1024. [CrossRef]

9. Malik, F.T.; Clement, R.M.; Gethin, D.T.; Krawszik, W.; Parker, A.R. Nature's moisture harvesters: A comparative review. *Bioinspiration Biomim.* **2014**, *9*, 031002. [CrossRef]
10. Sharma, D.K.; Pachchigar, V.; Ranjan, M.; Sikarwar, B.S. Plasma nano-patterning for altering hydrophobicity of copper substrate for moist air condensation. *Appl. Surf. Sci. Adv.* **2022**, *11*, 100281. [CrossRef]
11. Clus, O.; Ouazzani, J.; Muselli, M.; Nikolayev, V.; Sharan, G.; Beysens, D. Comparison of various radiation-cooled dew condensers using computational fluid dynamics. *Desalination* **2009**, *249*, 707–712. [CrossRef]
12. Beysens, D.; Brogginib, F.; Milimouk-Melnytchoukc, I.; Ouazzanid, J.; Tixiere, N. New Architectural Forms to Enhance Dew Collection. *Chem. Eng.* **2013**, *34*, 79–84.
13. Reinhardt, D. Regulation of phyllotaxis. *Int. J. Dev. Biol.* **2005**, *49*, 539. [CrossRef] [PubMed]
14. Reinhardt, D.; Pesce, E.-R.; Stieger, P.; Mandel, T.; Baltensperger, K.; Bennett, M.; Traas, J.; Friml, J.; Kuhlemeier, C. Regulation of phyllotaxis by polar auxin transport. *Nature* **2003**, *426*, 255–260. [CrossRef]
15. Nobel, P.S. *Environmental Biology of Agaves and Cacti*; Cambridge University Press: Cambridge, UK, 2003.
16. Ju, J.; Bai, H.; Zheng, Y.; Zhao, T.; Fang, R.; Jiang, L. A multi-structural and multi-functional integrated fog collection system in cactus. *Nat. Commun.* **2012**, *3*, 1247. [CrossRef] [PubMed]
17. Schill, R.; Barthlott, W.; Ehler, N. Cactus spines under the electron scanning microscope. *Cact. Succ. J.* **1973**, *45*, 175–185.
18. Malik, F.; Clement, R.; Gethin, D.; Beysens, D.; Cohen, R.; Krawszik, W.; Parker, A. Dew harvesting efficiency of four species of cacti. *Bioinspiration Biomim.* **2015**, *10*, 036005. [CrossRef]
19. Malik, F.; Clement, R.; Gethin, D.; Kiernan, M.; Goral, T.; Griffiths, P.; Beynon, D.; Parker, A. Hierarchical structures of cactus spines that aid in the directional movement of dew droplets. *R. Soc. Philos. Transl. A* **2016**, *374*, 20160110. [CrossRef] [PubMed]
20. Larridon, I.; Walter, H.E.; Guerrero, P.C.; Duarte, M.; Cisternas, M.A.; Hernández, C.P.; Bauters, K.; Asselman, P.; Goetghebeur, P.; Samain, M.S. An integrative approach to understanding the evolution and diversity of Copiapoa (Cactaceae), a threatened endemic Chilean genus from the Atacama Desert. *Am. J. Bot.* **2015**, *102*, 1506–1520. [CrossRef]
21. Malik, F. A Study of Dew Harvesting Cacti to Inform the Development of a Biomimetic Inspired Water Collection Device. Ph.D. Thesis, Swansea University, Wales, UK, 2016.
22. Beysens, D.; Broggini, F.; Milimouk-Melnytchouk, I.; Ouazzani, J.; Tixier, N. Dew architectures—Dew annouces the good weather. In Proceedings of the Confèrence Internationale mc-2012 "Matèrialitès Contemporaines", Les Grands Ateliers, Villefontaine, France, 30 November 2012.
23. Maestre-Valero, J.F.; Martinez-Alvarez, V.; Baille, A.; Martín-Górriz, B.; Gallego-Elvira, B. Comparative analysis of two polyethylene foil materials for dew harvesting in a semi-arid climate. *J. Hydrol.* **2011**, *410*, 84–91. [CrossRef]
24. Nilsson, T.M.J.; Vargas, W.E.; Niklasson, G.A.; Granqvist, C.G. Condensation of water by radiative cooling. *Renew. Energy* **1994**, *5*, 310–317. [CrossRef]
25. Medici, M.-G.; Mongruel, A.; Royon, L.; Beysens, D. Edge effects on water droplet condensation. *Phys. Rev. E* **2014**, *90*, 062403. [CrossRef]
26. Trosseille, J.; Mongruel, A.; Royon, L.; Beysens, D. Effective substrate emissivity during dew water condensation. *Int. J. Heat Mass Transf.* **2022**, *183*, 122078. [CrossRef]
27. Meng, Y.; Dang, Y.; Suib, S.L. Materials and devices for atmospheric water harvesting. *Cell Rep. Phys. Sci.* **2022**, *3*, 100976. [CrossRef]
28. Beysens, D. Estimating dew yield worldwide from a few meteo data. *Atmos. Res.* **2016**, *167*, 146–155. [CrossRef]
29. Gao, L.; Mccarthy, T.J. Contact angle hysteresis explained. *Langmuir* **2006**, *22*, 6234–6237. [CrossRef]
30. Park, K.-C.; Kim, P.; He, N.; Aizenberg, J. Condensation on Slippery Asymmetric Bumps. *arXiv* **2015**, arXiv:1501.03253. [CrossRef]
31. Yetman, D. *The Great Cacti: Ethnobotany & Biogeography*; University of Arizona Press: Tucson, AZ, USA, 2007; p. 31.
32. Baghel, V.; Sikarwar, B.S.; Muralidhar, K. Dropwise condensation from moist air over a hydrophobic metallic substrate. *Appl. Therm. Eng.* **2020**, *181*, 115733. [CrossRef]
33. Kidron, G.J. The effect of substrate properties, size, position, sheltering and shading on dew: An experimental approach in the Negev Desert. *Atmos. Res.* **2010**, *98*, 378–386. [CrossRef]